Mapping of Reservoir Facies within Heterogeneously Deposited and Structurally Deformed Strata in Tripura Frontal Fold Belt of Assam and Assam Arakan Basin: Application of Sequence Stratigraphy, 3D Seismic Attributes and Inversion*

Hari Lal[1], N.P. Singh[1], and A.K. Tandon[1]

Search and Discovery Article #30255 (2012)
Posted November 19, 2012

*Adapted from extended abstract prepared in conjunction with oral presentation at AAPG International Conference and Exhibition, Singapore, September 16-19, 2012, AAPG©2012

[1]GEOPIC, ONGC, Dehradun, India (lal_hari@ongc.co.in)

Abstract

Identification and mapping of Late-Oligocene-Miocene-Pliocene reservoir sands in the Tripura frontal Fold Belt of Assam and Assam Ararkan Basin has been elusive due to relatively poor imaging caused by surface-logistics and subsurface complexities. The study area falls in the western part of a complex tectonic zone consisting of foreland basin setting initiated by collision and subduction of the Indian Plate beneath the Burmese Plate to the east. The subsequent compressional tectonics formed NNW-SSE to N-S elongated Tripura-Chittagong Fold Belt consisting of series of anticlines and synclines arranged in an en-echelon pattern. The sandstones of Bhuban Formation of Miocene age are gas bearing in both the anticlinal and synclinal parts.

The objective of this study was to map reservoir facies in intervening synclines by interpreting newly acquired 3D seismic data. To meet the objective, robust interpretation workflows consisting of data enhancement, sequence stratigraphic analysis, seismic attribute analysis, spectral decomposition, impedance inversion and seismic guided multi-attribute log property mapping were applied to bring out the sand dispersal pattern. The available logs and geologic data were used for calibration and validation at the different stages of interpretation.

The enhancement in signal-to-noise ratio and continuity were achieved through spatial filters which minimized the acquisition footprints and random noise in 3D seismic. Sequence stratigraphic analysis consisted of identification of basin setting (mostly from

published data), paleodepostional environments (from published data, log motifs and seismic) and sequence stratigraphic framework building from identification of stratal terminations and chronostratigraphic surfaces in 3D seismic.

Dip-azimuth, coherency and volumetric curvature attributes provided detailed geomorphology which was interpreted in terms of depositional environments. Attribute-based anomalies in linear to lobe-like geometries are observed to be aligned in the northeast-southwest direction. The stratal terminations, retrogradational and progradational stacking patterns indicate constructive and destructive deltaic systems deposited under transgression-regression cycles. The provenance is interpreted towards north to northeast. Gas sands are found in both regressive as well as in transgressive sandstone reservoirs.

Introduction

The study area is located in a tectonically active geologic province of the Assam-Arakan Fold Belt (AAFB) in the western part of Tripura state in India. The Fold Belt is oriented mainly in a north-south direction and is spread over the states of Tripura and Assam of India and eastern Bangladesh (Figure 1). The province has prolific gas producing fields (e.g., Baramura, Agartala Dome, Rokhiya, Adamtila, etc. in India, and Titas, Habigunj, Fenchufunj, etc. in Bangladesh) in Bhuban-Bokabil sandstone reservoirs of Miocene-Pliocene age. Initially fault bounded structures mapped with surface geology and 2D seismic data were considered as viable entrapment models, but these met with many surprises, mainly due to absence of envisaged reservoir facies (sandstone). Well log interpretations show sudden lateral facies change from sand to shale within a very short distance and thus indicating heterogeneous depositional patterns. Episodic compressional forces resulting from subduction/thrusting and uplift towards the east, northeast and north created multistage deformation in the strata.

For mapping and delineation of reservoir facies and updating geologic models, 3D seismic data were acquired over different prospects. We have interpreted 3D data sets of three vintages (Northern, Middle and Southern) covering about 1000 km2 area in the western part of the fold belt in Tripura (Figure 1). As the basin evolved through various tectonic phases resulting in different structural styles (passive extensional to collision, subduction and thrusting), depositional environments (shelf/slope to trenches and flexures), depositional processes (fluvio-deltaic to gravity slides to fluvial intermontane), sediment supply and accommodation, mapping of reservoir facies within this basin is relatively difficult as compared to basins with simpler tectonic settings (e.g. passive margin basins). To meet the objective, robust interpretation workflows consisting of sequence stratigraphic concepts and 3D seismic attribute analyses were applied. Prior to interpretation, data enhancement techniques were used, as seismic data is relatively poor due to surface logistics and subsurface complexities. Well logs and other geologic data were integrated for calibration, validation and seismic guided multi-attribute log property mapping. Details of interpretation procedure and results are described in this article.

Tectonic Setting and General Geology

The Assam-Arakan Fold Belt (AAFB) is in the eastern part of the Assam and Assam Arakan Basin, with current peripheral foreland basin setting resulting from the collision of the Indian Plate with Burmese Plate during Oligocene to Late Miocene. Pre-collision phases (Paleozoic to Early to Middle Eocene) are represented by rift, drift to passive continental margin type setting with Tripura-Cachar falling in the slope to deep marine environment. The foreland setting was initiated by subduction of the Indian Plate below Eurasian Plate (Burmese Platelet) and formation of the Indo-Burmese ranges. Post Oligocene sedimentation is mainly controlled by syn- and post-orogenic depositional processes.

The general stratigraphy of the area is well documented in published literatures (Curiale et al., 2002; Kale et al., 2007). Stratigraphy of post-Oligocene sequences is mainly based on surface geologic mapping and drilled wells (Figure 14). Different sedimentary units are exposed along the narrow linear ranges. Pre-Surma formations are not exposed in the area and Post-Tipam formations are mainly eroded from the anticline and are present in the subsurface within the broad synclines. Pre-Surma is also not penetrated by any drilled well. The Bokabil Formation of Late Miocene age overlies the Bhuban Formation and is underlain by the Tipam Sandstone Formation of the Tipam Group of Early Pliocene age. The Bokabil Formation mainly consists of alternations of argillaceous and arenaceous deposits in delta front settings, in regressive condition which subsequently resulted in fluvial environment during the deposition of over-lying Tipams. The Bhuban Formation is divided into three members: Lower, Middle and Upper. The lower part of the Lower Bhuban contains lenticular conglomerates. The middle part is mostly argillaceous and the upper part is mostly alternations of thick beds of sandstones and shales. The sediments are mainly shales, sandy shales and siltstones. Occasional conglomerates and lenticular sandstones are also present. The Upper Bhuban is dominantly arenaceous. Paleontological and palynological studies in the area have indicated that Lower Bhuban to Lower Bokabil sediments were deposited in cyclic fluctuating marine to marginal marine environments in an overall deltaic setting (Biswas, 1984). The Bhuban Formation is the focus of this article.

Data Enhancements

In the area, due to difficult surface logistics and complex subsurface geology, reflections are found to be contaminated by acquisition footprints and random noise. For enhancing signal-to-noise ratio and continuity, and minimizing acquisition foot prints, spatial filters were applied. Original and filtered vertical sections and time slices, in the northern area, are compared in Figure 2. Reduction in random noise and enhancement in continuity and standout are clearly seen on filtered sections/slices.

Sequence Stratigraphic Framework

In seismic data interpretation, initial framework built with sequence stratigraphic considerations is very effective for seismic attribute analysis and deciphering structural and stratigraphic features hidden in the seismic data. Broadly, stratigraphic surfaces are classified into three types: sequence boundary, system tract boundary, facies contacts within system tract (Catuneanu, 2008). Stratigraphic surfaces may be environment dependent (fluvial incision, transgressive wave ravinement, etc.), geometric surface (defined by stacking pattern and stratal terminations) and depending on environment and or geometry both (e.g., maximum flooding surface (MFS), Maximum regressive surface (MRS)). Stratigraphic surfaces can be identified from regional continuous data (seismic, outcrops). Discrete data, small outcrops, well logs, cores and other geologic data are also used in framework building by tying seismic events with established stratigraphic markers. In the present context, seismic data is localized in a small geologic area (shelfal part of basin) hence reflection pattern and terminations (progradational clinoforms, downlap, toplap, onlap, etc.) are identifiable only in a few deeper parts where truncations, erosional surfaces and amplitude based reflection packages are scantly seen. Sequence stratigraphic surfaces were identified by integrating seismic, well logs and other information available in the literature/reports of the area (e.g. ONGC PS Cube report 2007; Kale et al., 2007).

The sequence stratigraphy of the encountered Mio-Pliocene successions in the well and outcrops of Tripura Fold Belt is well document in the PS Cube report 2007. Sediments older than Mio-Pliocene are not exposed or penetrated in the subsurface. In the Tripura Fold Belt area, no 1st order sequences have been identified. The Mio- Pliocene sediments are classified into two 2nd order sequences named as the first 2nd order and the second 2nd order foredeep sequence. A regionally correlatable sub-aerial unconformity CII 100 separates the first 2nd order sequence below from the second 2nd order sequence above (Fig. 3a). The bottom of First 2nd Order sequence (i.e., sequence boundary) is neither penetrated by any drilled wells nor it is visible
in the seismic section of the area. In this paper we are analysing only HST of first 2nd Order sequence bounded by 2nd order MFS at bottom and 2nd Order sequence boundary (CII100) at top. A representative seismic section along with overlay of GR (gamma ray) and LLD (resistivity) logs is shown in Figure 3a. Seismic section shows alternating strong amplitude reflection package (SARP), weak amplitude reflection package (WARP), cut-features, erosional surfaces and variations in attitudes of reflection events. Log motifs are also changing between fining upward, coarsening upward, and sometimes aggrading cylindrical. Based on seismic and log characteristics, seven surfaces of sequence stratigraphic significance are correlated on the section. Surfaces are named as FD-1 2nd Order MFS (Maximum flooding surface), WRS-6 (Wave ravinement surface), MFS-4, MRS-2 (maximum regression surface), MFS-6, WRS-4 and CII100 2nd Order SB (sequence boundary). In the lithostratigraphy, WRS-6 is just below the Lower Bhuban top, MRS-2 is just below Middle Bhuban Top and CII100 coincides with the Bhuban-Bokabil boundary.

Deformations of strata are seen throughout the sedimentary succession. The isochron map of CII100 (Figure 3b) shows a central high trend in arcuate shape from north to south with convexity towards the east. The high trend is separated from lows towards east and west by reverse faults. The northern part is relatively flat and the southern part has prominent lows in the northwest and southeast. Lateral variation of seismic amplitude along CII100 is shown in Figure 3c. Amplitude anomalies are aligned in a northeast-southwest

oriented lobe to channel-like geometry. The anomalies along CII100 have been caused by facies changes in underlying (HST) and overlying (LST) layers. At well D, CII100 is at the top of thick sands.

Seismic Attribute Computation and Analysis

Seismic reflection signals and their derived attributes may be sensitive to changes in impedance, thickness of layers and/or texture and geomorphology. Amplitude-based attributes mainly depend on impedance in which rock and fluid properties (velocity, density, porosity saturation, etc.) are generally inherent. Frequency-based attributes generally depend on layer thickness, depositional cyclicity and absorption. Time based attributes, e.g. dip-azimuth and curvature, depend on geomorphology and texture.

Amplitude

Amplitude may be computed through complex trace analysis (reflection strength) or simply from magnitude of samples by various averaging/selection (RMS, maximum peak or trough amplitude, etc.). As amplitude is sensitive to impedance contrast, and impedance is related to rock and/or fluid properties, the amplitude attribute tells about variation in rock and fluid properties. However, geometrical effects (e.g. tuning) may also generate high amplitude. Finding interrelationships between impedance and lithology (sand, shale) and reservoir properties (porosity, saturation, etc.) is helpful in inferring the rock/fluid properties from the amplitude. The cross plots between impedance and gamma ray (mainly lithology log) have shown varying impedance for sands and shales (Figure 4a) with large overlaps. However, impedance contrast between gas-sands and shale is strongly negative in two gas-bearing wells (Figure 4b). When contrast is strong, high amplitude reflections are generated and when it is insignificant, reflections from sands are not recognized. Thus, occurrence of amplitude anomaly is generally related to sands in an overall shale background, though there may be some other sands which may be hidden to amplitude changes. Horizon slices (reflection amplitude or any attribute extracted along and/or parallel to correlated horizons) are most effective for stratigraphic interpretation (Brown, 2004). The reflection strength section and successive horizon slices of CII100 horizon in the northern area are given in Figure 5.

Spectral Decomposition

In spectral decomposition, amplitude and phase are computed at discrete frequencies. The lateral changes in amplitude may depend on the thinning or thickening of strata, geomorphology along the interfaces and absorption within layers. This can be used for thickness prediction (Partyka et al., 1999), geomorphology (channels, subtle faults, etc.) (Marfurt and Kirlin, 2001) and direct detection of hydrocarbons (Castagna et al., 2003). Spectral decomposition horizon slices of CII100 at 13 Hz and of MRS-2 at 15 Hz, for southern area, are given in Figure 6**.**

Coherency

The coherence attribute measures lateral changes in seismic waveforms and amplitude and is very effective for mapping of channels, faults and other subtle discontinuities in a 3D data set. Coherency horizon slices computed along CII100 and MRS-2 show faults and other discontinuities (Figure 7**)**.

Dip-Azimuth

Dip and azimuth is computed either from seismic reflection events or horizons, and are helpful in detecting faults and fractures. Dips measures the magnitude of dip and azimuth gives the direction of dip from travel time. Dip-Azimuth (DAT) is displayed simultaneously. Dip-azimuth slice of CII100 and MRS-2 surfaces are given in Figure 8. Maps are interpreted with the help of a given colour bar which shows both azimuth (four colour bands) and magnitude of dip from the change in intensity of colour within bands. Detailed geomorphology along the interpreted surface can be inferred from variations in dip and azimuth. Linear alignments of orthogonal dip direction (e.g. north direction within dominantly east direction) are indicative of cross-faults.

Curvature

Curvature is the second derivative of travel time computed along horizons or reflection events (volumetric curvature). Curvature shows the locations where the surface departs from a simple folded sheet due to warping or shattering of the surface (Blumentrit, 2006). These areas may be affected by fracturing. Most positive and most negative curvature slices along CII100 are given in Figure 9. Volumetric curvature attributes are valuable in mapping subtle flexures and folds associated with fractures in deformed strata (Chopra and Marfurt, 2007).

Acoustic Impedance Inversion and Multi-Attribute Log Property Mapping

As impedance is a layer property, by knowing the impedance of layers bounded by interfaces, we can directly predict the lithology and in favourable conditions the nature of fluids also. The generated impedance volume can be used as an external attribute for estimation of reservoir parameters (porosity, saturation, sand volume, etc.) by integrating logs and seismic attributes (Hampson et al., 2001). Acoustic impedance volume was generated through model-based post-stack inversion method in which the initial impedance model is prepared from actual impedance log and correlated horizons. Seismic guided log property mapping using Probabilistic Neural Network (PNN) was performed for estimation of porosity and sand volume (Sandvol). As in the areas where well control is inadequate (wells are clustered in the small part of area) and also synthetic to seismic matching is relatively poor, estimated impedance and reservoir parameters are used qualitatively. Areas with amplitude anomalies are showing relatively low impedance and high sand

percentage. The northern area is relatively flat and here time slices can also represent stratal/horizon slices. Time slice at 1920 ms of reflection strength and sand volume along with impedance section with overlay of seismic trace are given in Figure 10. In this time range sands are of lower impedance than shales and generating high amplitude reflections.

Discussion

Depositional heterogeneity, post depositional structural deformation and relatively poor imaging create confusion in identification and mapping of stratal patterns and environmental analysis which may be used for inferring sand-rich intervals and areas. Geometrical relationships (e.g., downlap, toplap) between strata and stratigraphic surfaces become confusing due to folding, faulting and tilting. The limit of seismic resolution also creates confusion between toplap and terminations. Faulting and depositional/erosional processes both bring entirely different types of lithofacies in contact. Due to stratigraphic variations (e.g. lateral facies change and corresponding change in reflection character, cut-outs, etc.), correlation of surfaces and hence structural mapping become difficult. Similarly, structural variations (e.g. faulting, folding, tilting, etc.) pose problems in identification of stratigraphic features (channel-cuts, progradational clinoforms, etc.). Minimizing the impact of one factor onto another is the main key for inferring both structural and stratigraphic features simultaneously, for which horizon/stratal slices and flattened section/volumes with respect to correlated stratigraphic surfaces (horizons) have been used.

Maps and structural attributes of horizons (dip, azimuth, curvature) have given present day structural and geomorphic details. Physical attributes (wave shape, amplitude, frequency, etc.) computed along and/or within short windows with reference to horizons, have given geomorphic details and physical parameters which are least affected by structural deformation. Flattened seismic sections have helped in identification of stratal stacking and termination patterns.

Different types of stratal terminations (e.g. downlap, toplap), cut-outs and reflection characters (reflection strength, continuity, shape, etc.) have been observed in seismic section (Figure 3). Types of strata terminations can be related to changes in sea-level (e.g. onlap: transgression (rise), downlap/toplap: regression (fall)). Variations in reflection characters are related to lithologic/fluid contrasts. Normal and flattened sections are compared in Figure 11. Flattening has made recognition of geometrical relationship (e.g. toplap) easier in folded section. On a flattened section at MFS-6, oriented in a northeast-southwest direction across low in “southern” area (Figure 12**)**, various types of stacking patterns (progradational and retrogradational), termination patterns (downlap, toplap, truncation, erosion, incision) are interpreted in the upper part of Lower Bhuban and lower part of Middle Bhuban. MRS is recognized from toplap (progradational) and onlap (retrogradation) relationships of strata below and above it, respectively, in upper part of Lower Bhuban. This MRS surface is not seen in “middle” area (Figure 3).

The CII100 is deeply scoured. At places, scouring is so deep that even the sand layer below it is eroded and the preserved part of sand appear as a "relict" feature (Figure 13). Relict and cut features both are aligned parallel to the paleo-shoreline. Cuts are generally shale filled and act as good lateral seals. Vertical seal is provided by overlying shales. Due to cut, thickness of relict sand shows very sharp variation (from about 40-30 m to 0). Relict sands are quite extensive in the western part of "northern", "middle", "southern" area and are probed only in small part of "middle" area. Generally, amplitude variations on spectral decomposition frequency slices have associated variations in dip-direction on dip-azimuth map (Figure 13). In the southern area (Figure 12), overall progradation and progressive shift of paleo-shoreline southwest (down dip) towards the basinal side is interpreted in upper part of Lower Bhuban and lower part of Middle Bhuban. WRS-6 and MRS-2 form the lower and upper interfaces of a relatively low amplitude unit deposited, dominantly, under transgression within which channels are interpreted from attributes and log motifs. Within this unit, relatively thin gas-sands are found. Attribute slices (e. g. spectral decomposition amplitude slices at discrete frequencies) show deltaic lobe in Upper Bhuban (below CII100) and channels in Middle Bhuban (between WRS-4 and MRS-2) (Figure 6). Upper Bhuban sands (Regressive sands) generally are gas bearing in the top part with clear gas-water contact (GWC) and transgressive sands (Middle Bhuban) are gas bearing at multilevels in structurally favourable places. Structural and geomorphic details (faults, flexures, channels, lobes, etc) are mapped through coherency, dip-azimuth and curvature attributes (Figure 7, Figure 8 and Figure 9).

Conclusions

Seismic attributes within a sequence stratigraphic framework have been used for mapping structure, geomorphology and distribution of reservoir facies (sands) in the western Fold Belt of Tripura. Structure maps of surfaces and structural attributes (dip-azimuth, curvature) have shown deformation of strata both through tectonic and depositional processes. Deformations caused by tectonics are in the form of subsurface flexures, faults/thrust, anticlines and synclines. Deformations related to deposition are in the form of incision, truncation and erosion. Structural deformations are the main hindrance for mapping of depositional environment and facies because of confusion in recognition of stratal stacking and termination patterns. Impacts of structural deformation are minimized through volume flattening and attribute analysis along stratigraphic surfaces and within short time windows. Stratigraphic surfaces are generally cut by waves and thus making "relict" and "cutfill" features. The older relicts are dominantly sandy and younger fills are dominantly shaly. Geometries of attribute anomalies show lobe and channel-like features. Lobes are common in the Lower (below WRS-6) and Upper Bhuban (between CII100 and MRS-2) and channels are common in the Middle Bhuban (between MRS-2 and WRS-4). Stratal stacking and termination patterns and patterns of seismic facies variations have shown highstands (both progradation and aggradation) in the Lower and Upper Bhuban and transgressive conditions (retrogradation) in the Middle Bhuban.

Sands have varying acoustic properties and impedance contrast (strong negative to near zero) with respect to enclosing shales. Wherever contrast is strong and thickness is above the detectable limit, sands are generating bright spots. Thin and near-zero impedance contrast sands are not generating recognizable seismic signals even though they are commercial gas producers. Sands were

deposited in transgression-regression cycles. Regressive sands (high stand conditions) are generally thick and eroded at top of sequence and sands deposited during transgression are thin and intercalated with shales. Gas sands are found in both thick regressive as well as in thin transgressive reservoirs.

Acknowledgements

We express our sincere gratitude to Shri S.V. Rao, Director (E), ONGC, India, for according permission for submission and publication of this paper. We are thankful to Shri S.K. Das, Executive Director and former HOI, GEOPIC for assigning projects and valuable guidance, and Shri D. Sar, ED-HOI, GEOPIC for inspiration and encouragement towards submission of this technical paper. Dr. Alok Dave, Dy. General Manager (Geol.), KDMIPE, ONGC, is thankfully acknowledged for sharing his expertise on sequence stratigraphy and providing valuable suggestions for enhancing the quality of paper. The views expressed in this article are exclusively of the authors and need not necessarily match with official views of ONGC.

Selected References

Biswas, S.K., 1984, Stratigraphic investigation in Tripura Cachar region: Joint project by KDMIPE, CRBC, ERBC, ONGC. Unpublished report.

Blumentritt, C.H., and B. Stinson, 2006, Volume Based Curvature Analysis Illuminates Fracture Orientations, Fort Worth Basin, Texas: AAPG Search and Discovery Article #90052. (Abstract).
Brown, A.R., 2004, Interpretation of three-dimensional seismic data: AAPG Memoir 42, SEG investigation in Geophysics, v. 9, p. 517-529.

Castagna, J.P., S. Sun, and R.W. Siegfried, 2003, Instantaneous spectral analysis; detection of low-frequency shadows associated with hydrocarbons: The Leading Edge, v. 22/2, p. 120, 122, 124-127.

Catuneanu, O., 2008, Principles of sequence stratigraphy: Elsevier, Amsterdam, 375 p.

Chopra, S., and K.J. Marfurt, 2007, Volumetric curvature attributes add value to 3D seismic data interpretation: The Leading Edge, v. 26/7, p. 856-867.

Curiale, J.A., G.H. Covington, A.H.M. Shamsuddin, J.A. Morelos, and A.K.M. Shamsuddin, 2002, Origin of Petroleum in Bangladesh: AAPG Bulletin, v. 86/4, p. 625-652.

Hampson, D.P., J.S. Schuelke, and J.A. Quirein, 2001, Use of multiattribute transforms to predict log properties from seismic data: Geophysics, v. 66/1, p. 220-236.

Kale, A.S., P.K. Sinha, R.C. Agrawalla, G.K. Ray, and R.M. Baruah, 2007, Miocene-Pliocene Sequence Stratigraphy of Tripura, India and its Implication on Hydrocarbon Exploration: AAPG Bulletin, v. 91, p 75-84.

Marfurt, K.J., and R.L. Kirlin, 2001, Narrow-band spectral analysis and thin-bed tuning: Geophysics, v. 66/4, p. 1274-1283.

Partyka, G., J. Gridley, and J. Lopez, 1999, Interpretational applications of spectral decomposition in reservoir characterization: The Leading Edge, v. 18/3, p. 353-360.

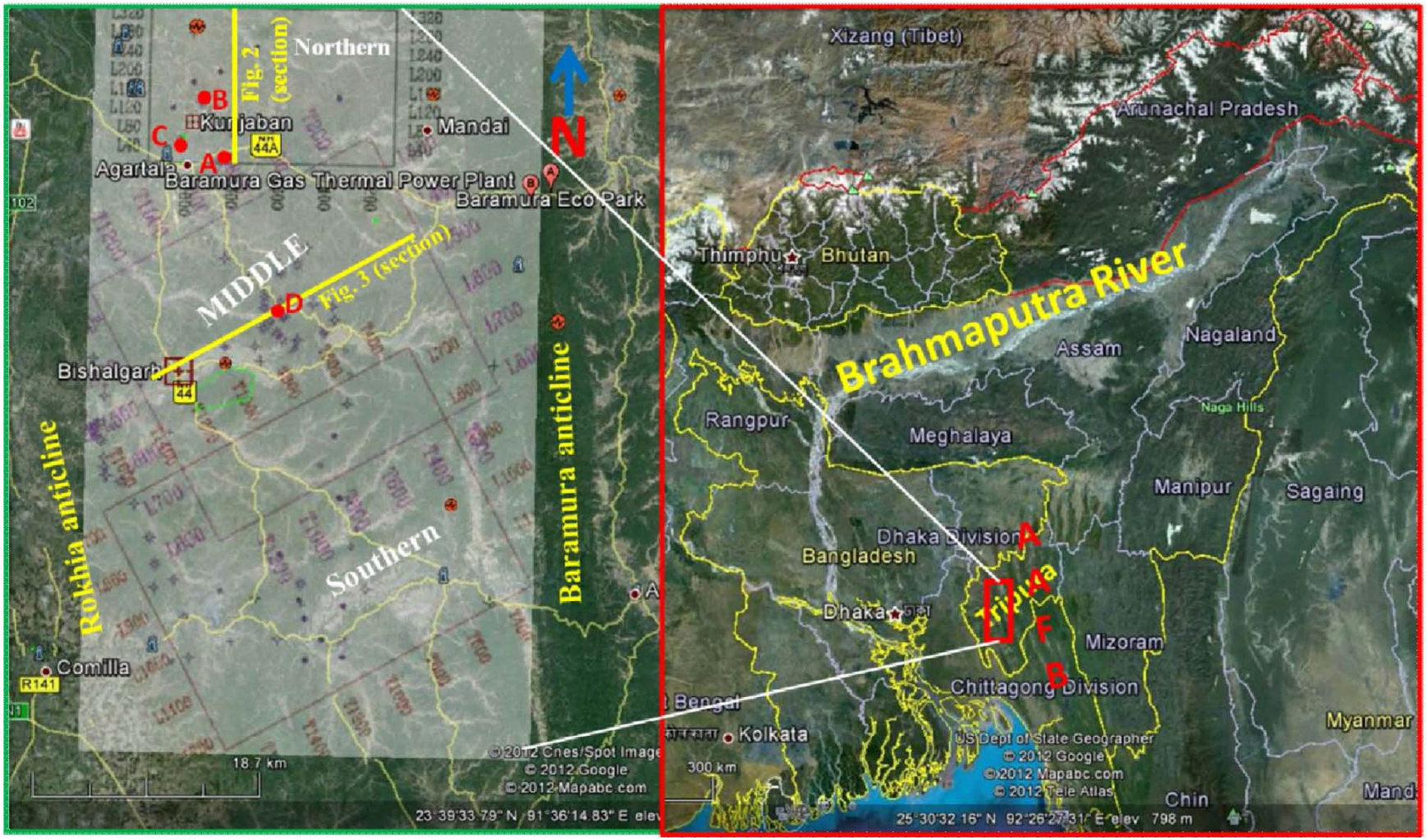

Figure 1. Index map of the area of study in Tripura Fold Belt. The area is covered by 3D surveys of three vintages (northern, middle, and southern) in a broad synclinal area.

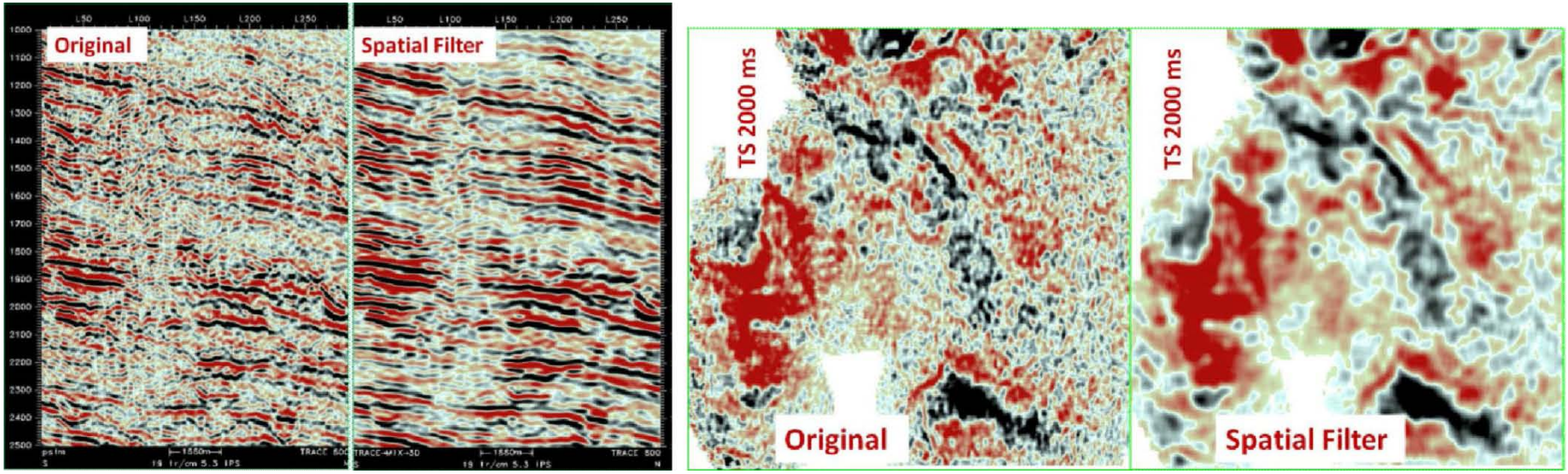

Figure 2. Seismic sections showing data enhancement through application of spatial filtering.

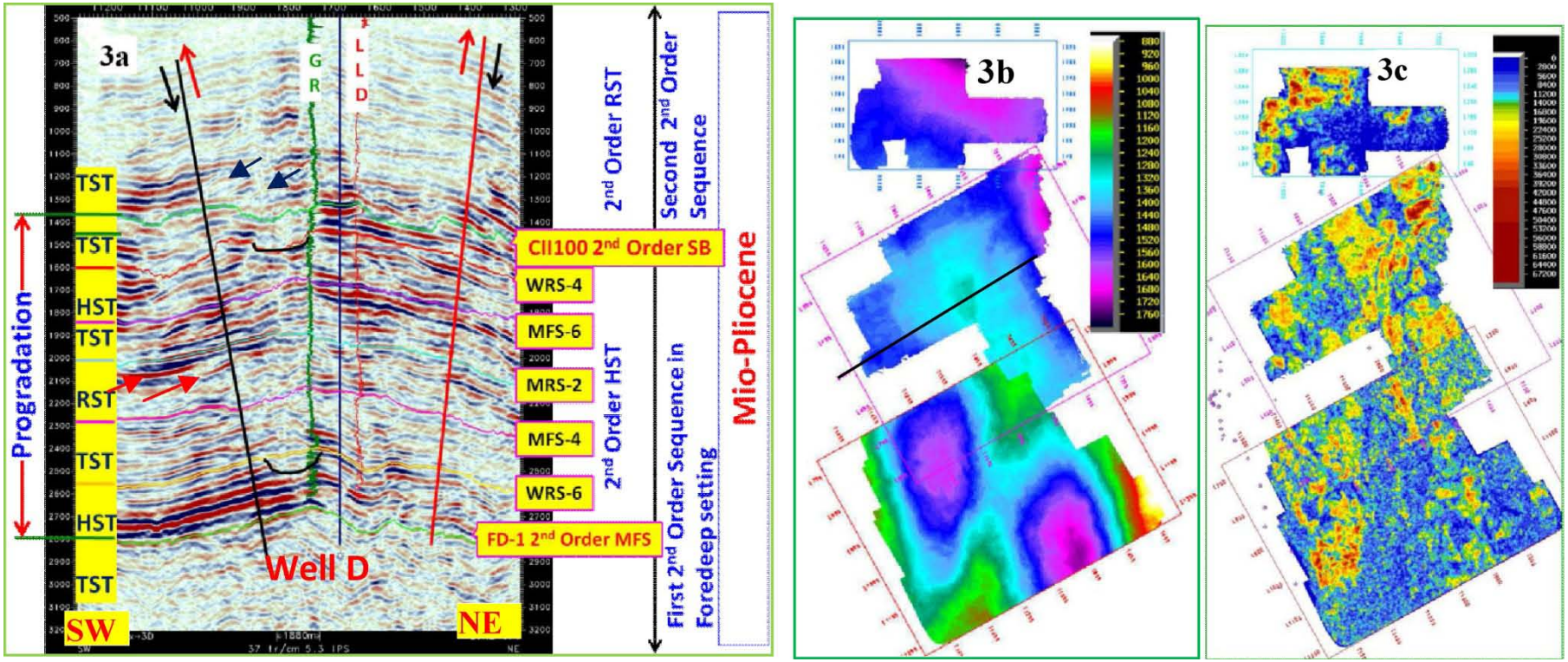

Figure 3. (a) Seismic section showing stratigraphic surfaces within Mio-Pliocene. (b) TWT map of CII100 (SB). (c) Amplitude map along CII100 (SB) surface.

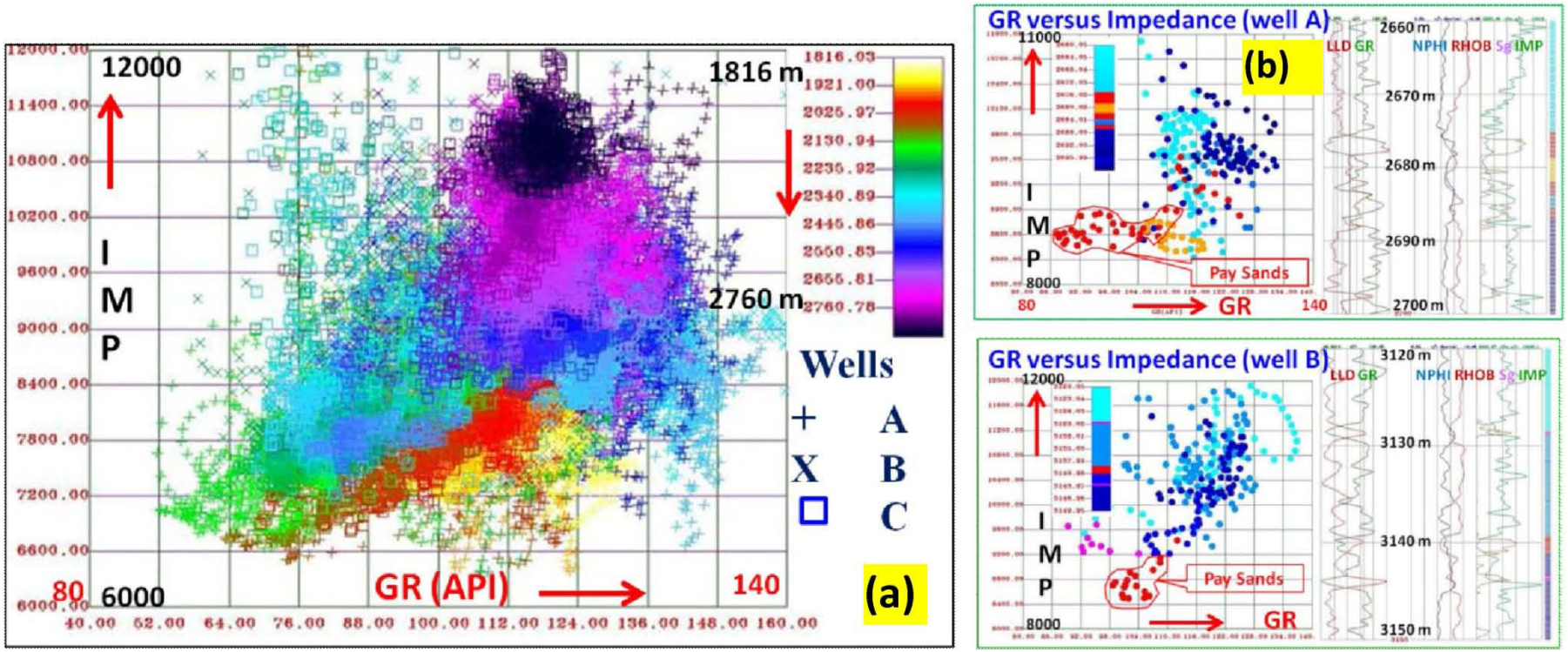

Figure 4. Cross-plot between gamma ray and impedance: (a) for three wells in the northern area, (b) for wells A and B focusing on the pay zones. In (b) points are colour coded with lithology: red: gas-sands; yellow: water sands; blue: shales.

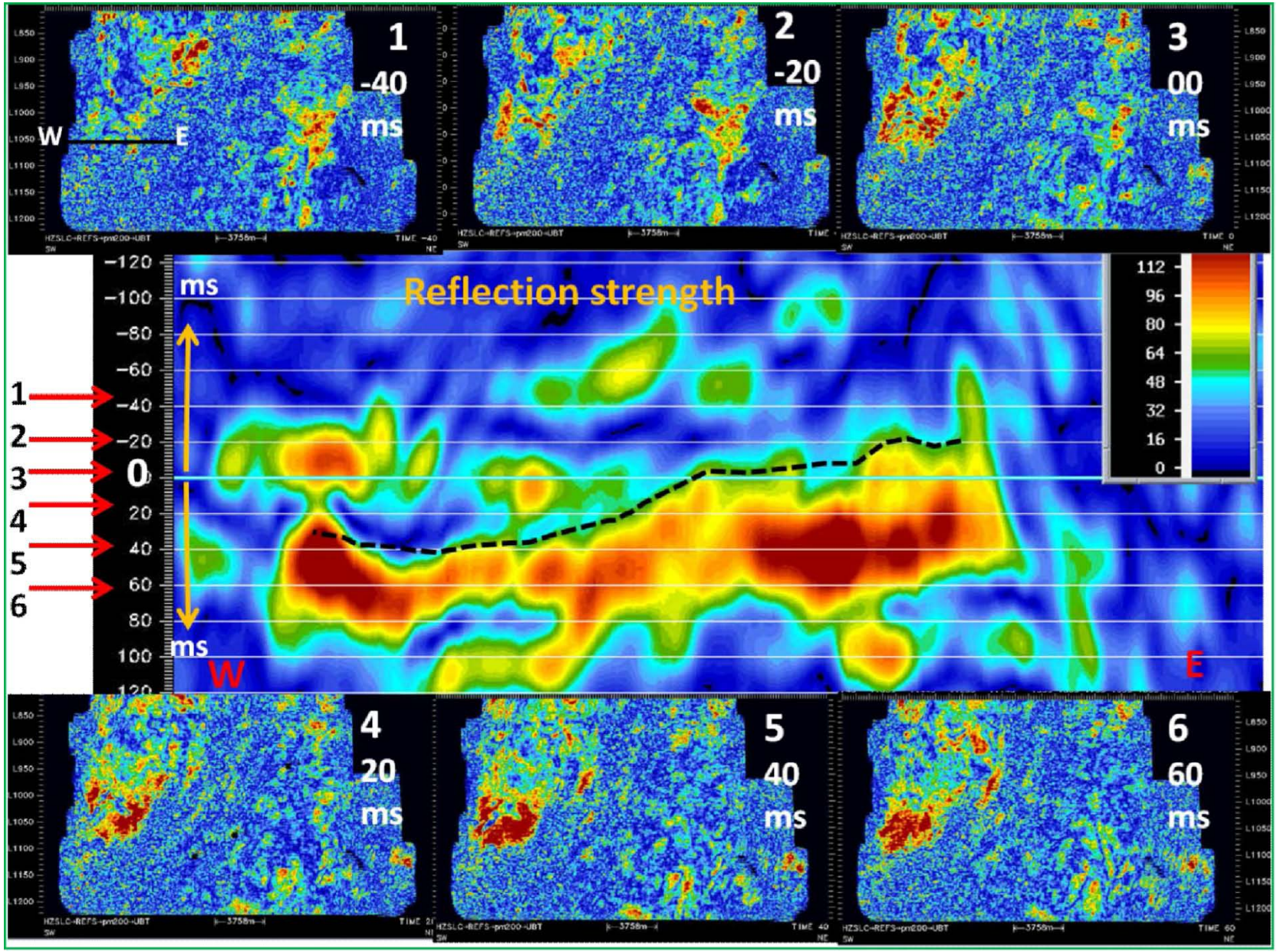

Figure 5. Horizon slices of reflection strength with reference to CII100 and flattened reflection strength section in northern area. Temporal positions of successive slices are shown on section with red arrows.

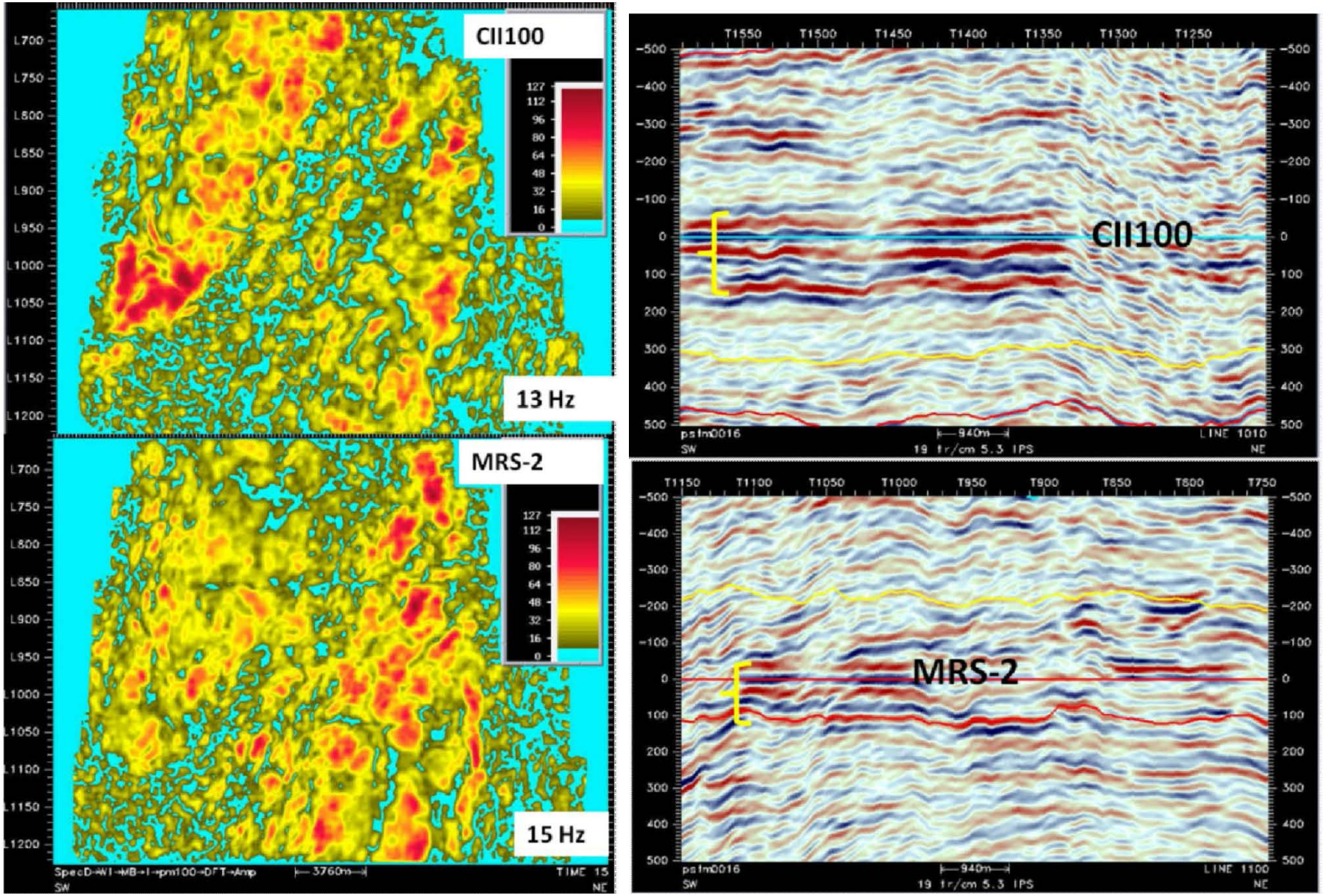

Figure 6. Spectral Decomposition frequency slices of amplitude focusing CII100 and MRS-2 surfaces in the southern area. Computation windows and seismic characters are shown on flattened vertical section with respect to CII100 and MRS-2 surfaces.

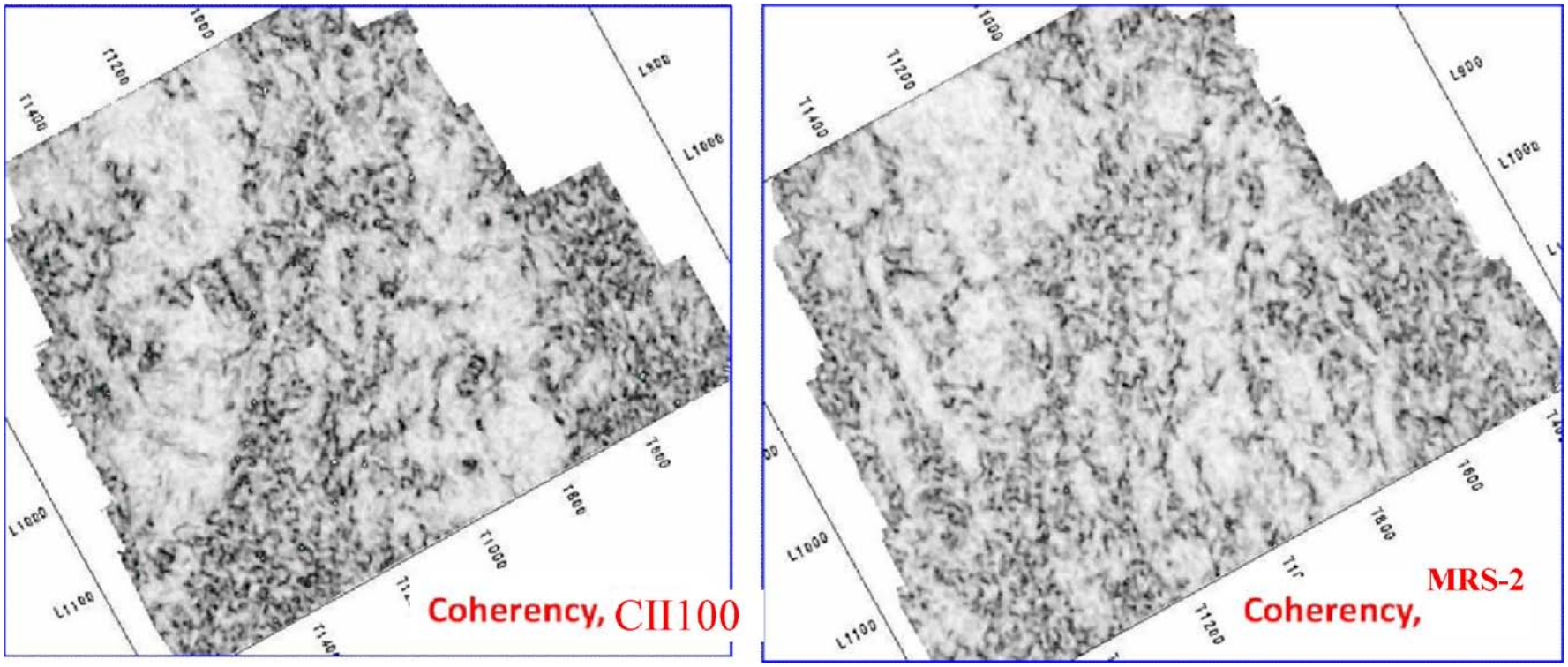

Figure 7. Coherency-horizon slices at CII100 and MRS-2 surfaces showing longitudinal, cross-faults and other discontinuities (southern area).

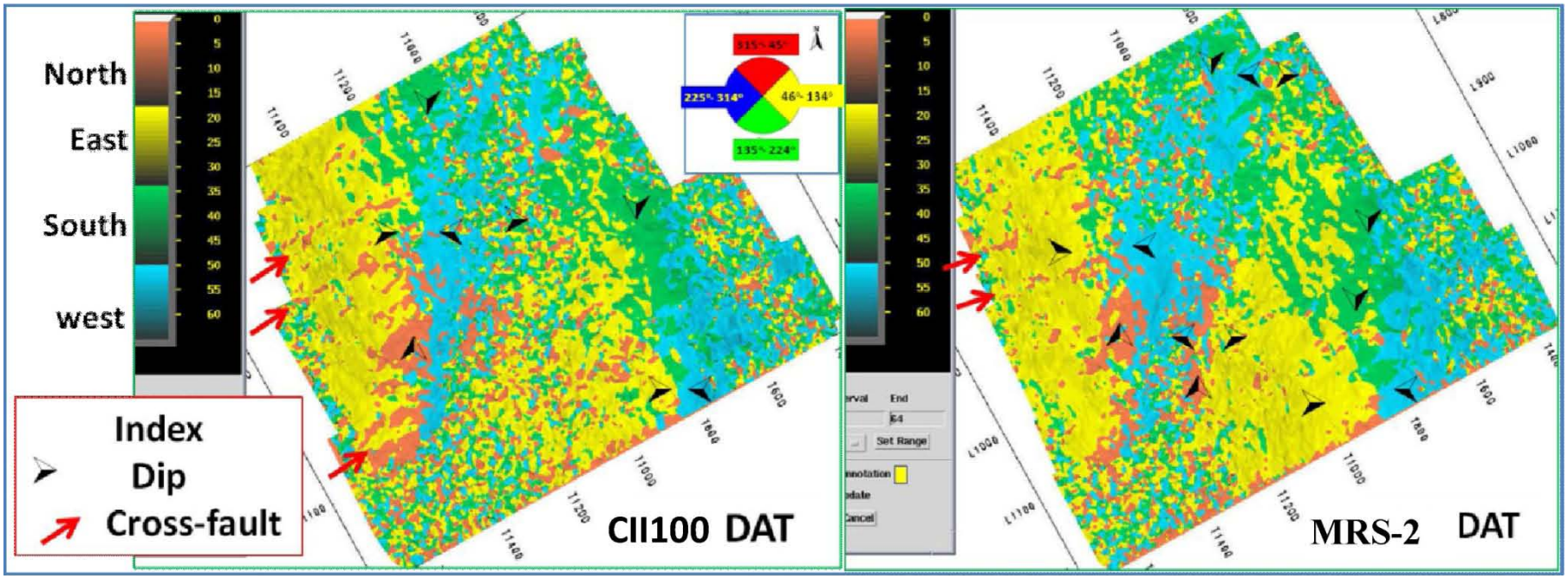

Figure 8. Dip-Azimuth slices at CII100 and MRS-2 surfaces showing faults and other geomorphic variations (southern area).

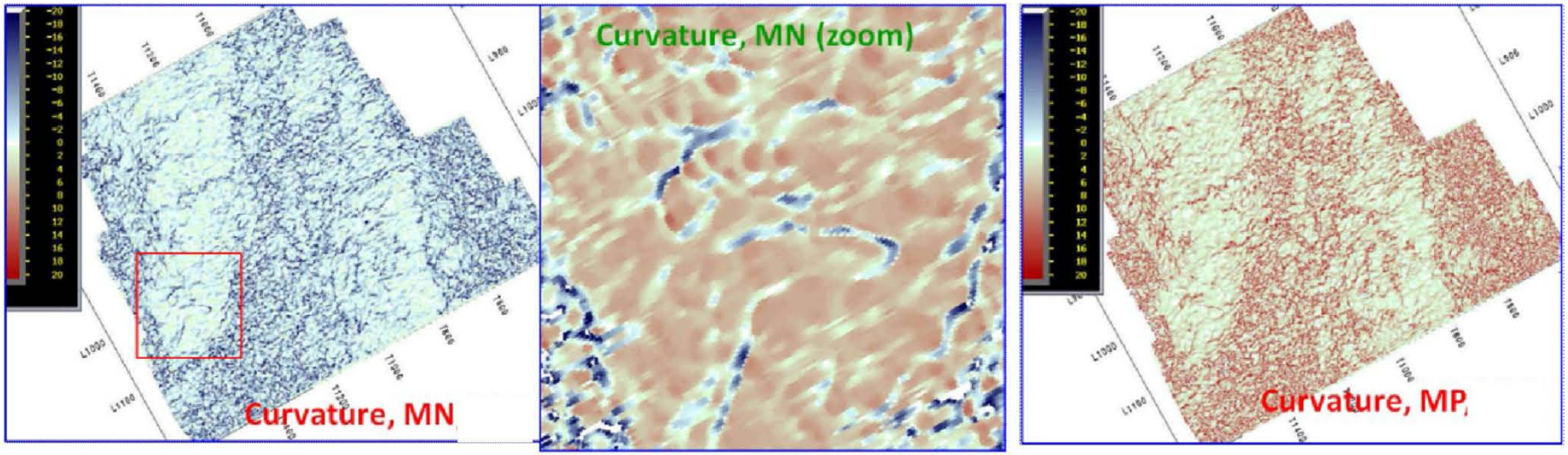

Figure 9. Most negative (MN) and most positive (MP) curvature at CII100 showing subtle faults flexures and channels (southern area).

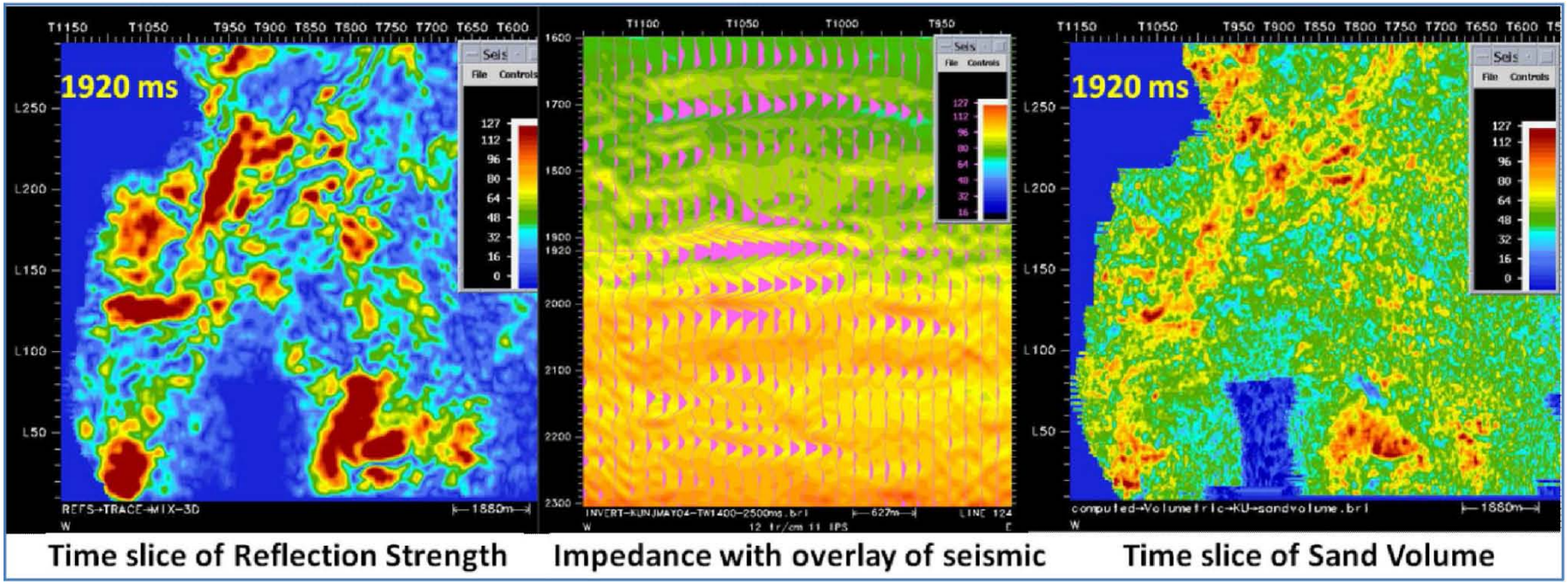

Figure 10. Time slices of reflection strength and sand-vol and impedance section with overlay of seismic trace.

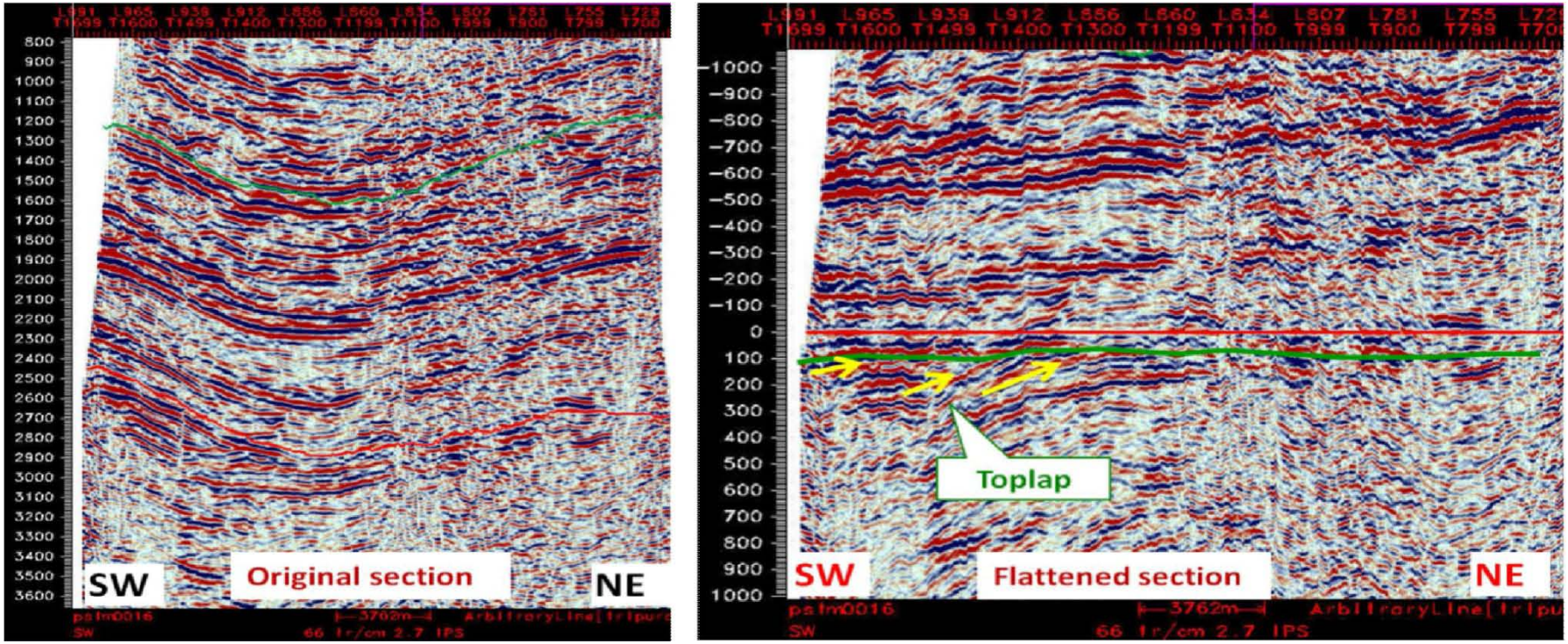

Figure 11. Flattening along a surface below WRS-6 showing stacking and ternination patterns.

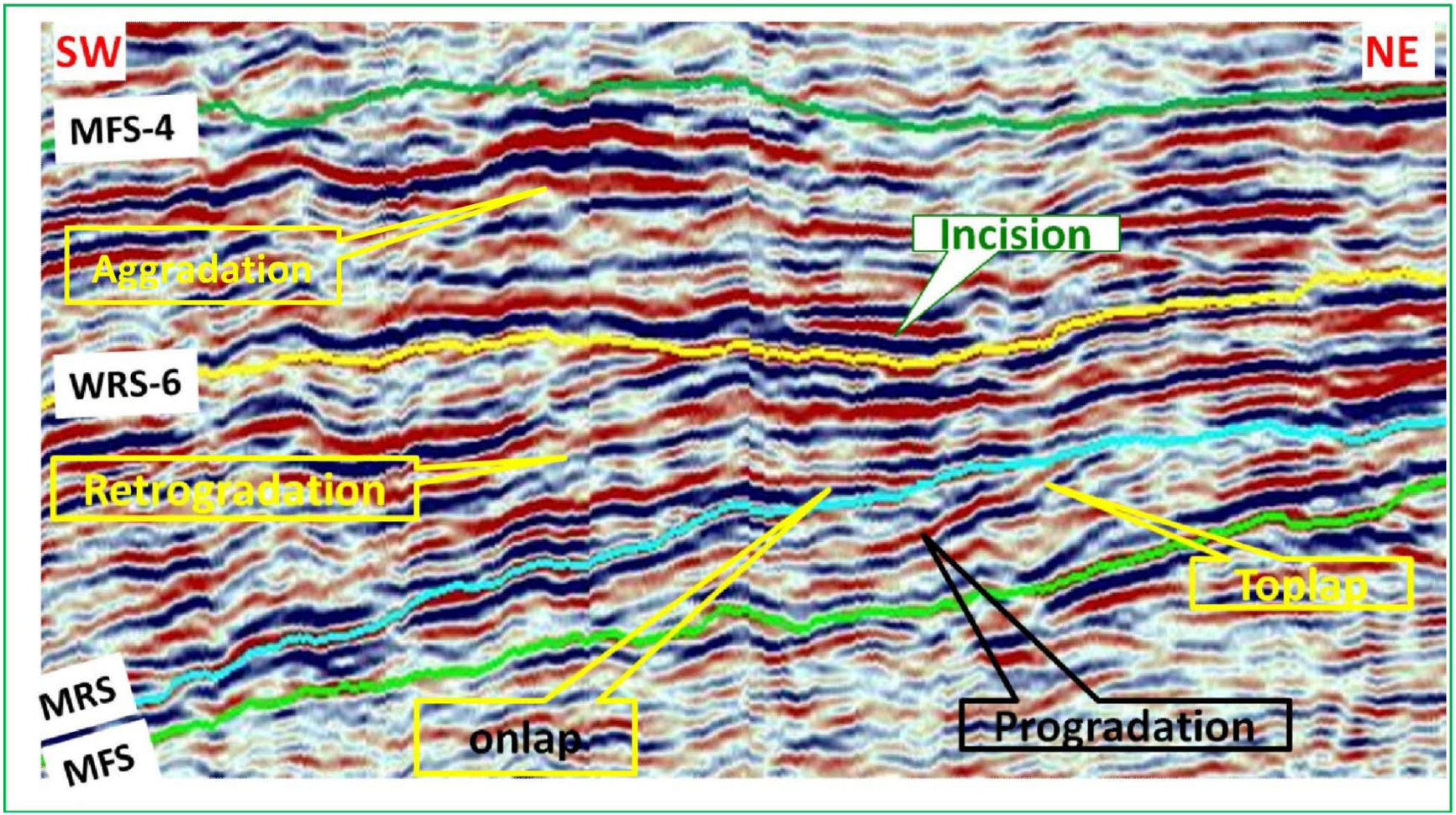

Figure 12. Stratal stacking and termination patterns within Lower Bhuban Formation. (Note: to make clinoforms and terminations more visible, horizontal and vertical scales are exaggerated and flattened surface (MFS-6) situated in upper part could not be shown).

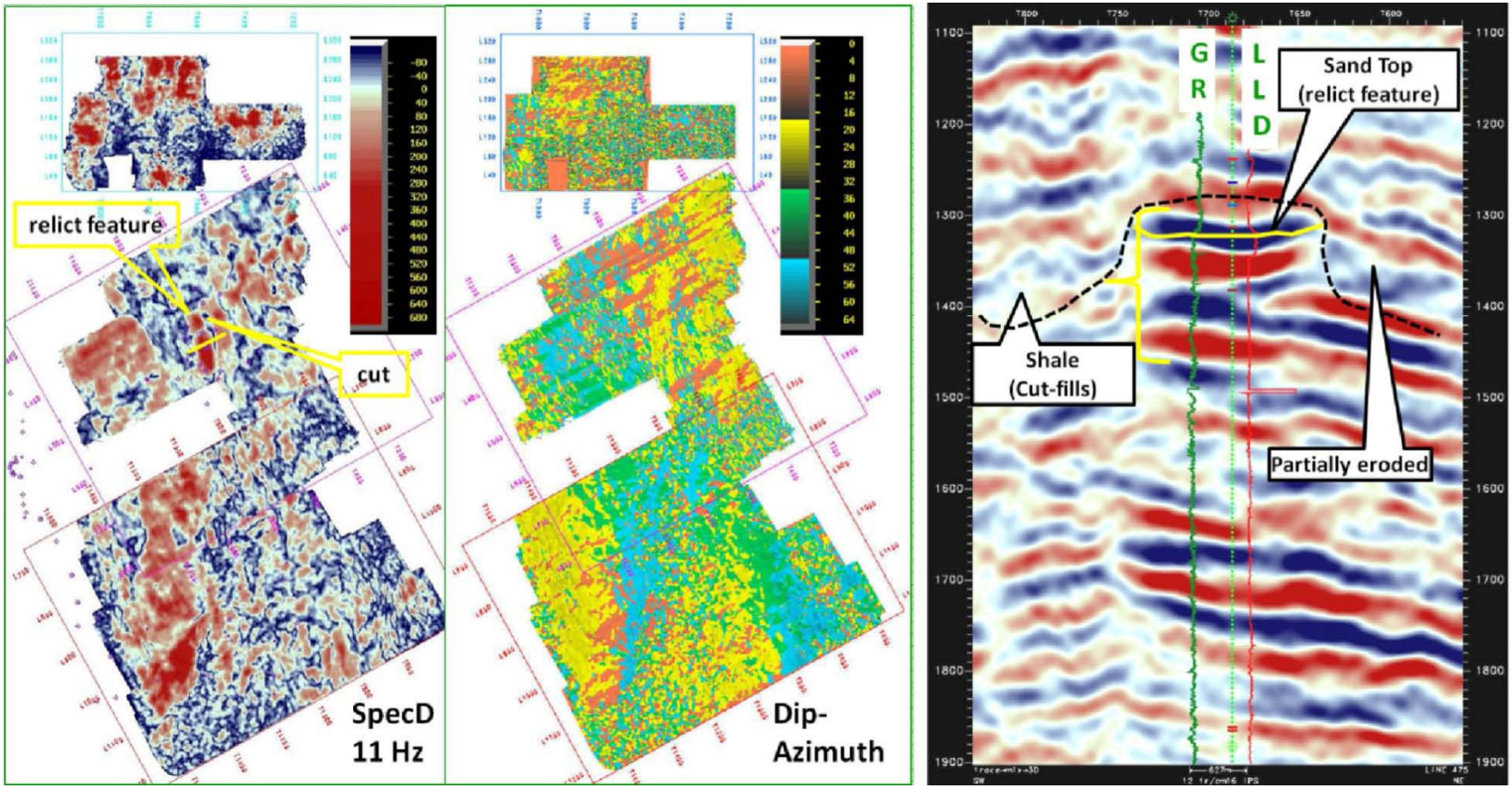

Figure 13. Spectral Decomposition and Dip-Azimuth maps at CII100 along with zoomed seismic section showing relict and cut features. High amplitude relict features in middle area show dip direction from northeast and cut features have dip direction from southwest.

Age	Group	Formation	Member	Thickness (m)	Tectonic history and phase	
Recent			Alluvium			
Pliestocene		Dihing		100-300		
		Dupitila	Upper	200-400		
Pliocene			Lower			
	Tipam	Girujan Clay		100-200		
		Tipam Sandstone		1500 (+)		
	Surma	Bokabill		1500	Uplift Himalayas	
		Bhuban	Upper Bhuban	1025	Major Himalayan Orogeny	Late Collision
Miocene			Middle Bhuban	1230		
			Lower Bhuban	2000 (+)	Subduction/Folding Indo-Burma	
Oligocene	Barail	Not penetrated			Early Collision India-Eurasia Tethys closing	Early collision

Figure 14. General stratigraphy of the study area.